

Impact of UAV Jittering on the Air-to-Ground Wireless Channel

Morteza Banagar, *Student Member, IEEE*, Harpreet S. Dhillon, *Senior Member, IEEE*,
and Andreas F. Molisch, *Fellow, IEEE*

Abstract—This letter studies the impact of unmanned aerial vehicle (UAV) jittering on the coherence time of the wireless channel between UAVs and a ground user equipment (UE), using a Rician multi-path channel model. We consider two different scenarios for the number of UAVs: (i) *single UAV scenario* (SUS), and (ii) *multiple UAV scenario* (MUS). For each scenario, we model the UAV jittering by two random processes, i.e., the Wiener and sinusoidal processes, and characterize the channel autocorrelation function (ACF) which is then used to derive the coherence time of the channel. For the MUS, we further show that the UAV-UE channels for different UAVs are uncorrelated from each other. A key observation in this letter is that even for a small UAV jittering, the coherence time of the channel may degrade quickly, which may make it difficult to track the channel and establish a reliable communication link.

Index Terms—Unmanned aerial vehicle, jittering, wireless channel, autocorrelation function, coherence time.

I. INTRODUCTION

UAVs have recently gained significant attention in wireless communications due to their fast and cost-efficient deployment, mobility, and high probability of line-of-sight (LoS) [1]. UAVs can be deployed as UEs to perform various tasks, such as package delivery, monitoring, and surveillance, or as wireless relays or even base stations to complement the coverage and capacity of terrestrial cellular networks [2]. Although the fast and easy deployment of UAVs is quite appealing for many applications, a significantly different operational regime motivates many fundamental questions. For instance, due to the lack of fixed and stable infrastructure and various environmental issues, such as bad weather conditions or wind gusts, UAVs may experience random fluctuations (also known as jittering) while hovering at a specific location [3]. Although these fluctuations are typically very small, they could severely affect the quality of the wireless channel because of the large values of the carrier frequency. Quite remarkably, the impact of UAV jittering on the properties of the air-to-ground wireless channel, such as its coherence time, has not been quantified in the literature yet, and is the main focus of this letter.

Prior Art. There has been a lot of recent interest in the analysis and design of UAV-assisted communication networks [4]–[10]. However, only a handful of them considered the

impact of random jittering of UAVs on the performance of the UEs. In [11], the authors studied the transmitter-receiver antenna mismatch caused by the random fluctuations of hovering UAVs in millimeter wave (mmWave) wireless communications. The problem of resource allocation in a drone cellular network when the UAVs are equipped with uniform linear antenna arrays and are also jittering is studied in [12] and further extended to planar antenna arrays in [13]. In these works, the authors designed algorithms to minimize total power consumption in a multiple-input single-output (MISO) system by jointly optimizing the UAV trajectory and transmit beamforming vector. Taking UAV jittering into account, the authors in [14] investigated a wiretap aerial system where the problem of secure and energy-efficient communication between a UAV and a ground UE is analyzed. Although these works address important problems related to UAV jittering, its impact on the wireless communication channel still remains an open problem, which is the main focus of this letter. Our contributions are summarized next.

Contributions. In this letter, we assume a Rician multi-path channel model and consider two scenarios for the number of UAVs: (i) SUS, where a single UAV communicates with the UE, and (ii) MUS, where multiple UAVs form a distributed multiple-input multiple-output (MIMO) transceiver to communicate with the ground UE. We then model the jittering behavior of the UAVs by two random processes, i.e., the Wiener process and the sinusoidal process. For the SUS, we rigorously characterize the channel ACF for both random processes and formulate the coherence time of the channel. We further derive the channel autocorrelation matrix in the MUS and demonstrate that the channels of different UAVs to the UE are uncorrelated from each other and the coherence time of these channels is the same as that of the SUS. One of the main outcomes of our analysis is that the coherence time of the channel is highly sensitive to UAV jittering. Specifically, even for small fluctuations of the UAV, the coherence time is small, which in turn makes the channel tracking and symbol detection very difficult. To the best of our knowledge, this is the first work that characterizes the impact of UAV jittering on the coherence time of the channel.

II. SYSTEM MODEL

We use the Cartesian coordinate system to represent the locations of the UAVs, the UE, and scatterers. For the number of UAVs, we consider two different scenarios: (i) SUS, where a single UAV is deployed at some arbitrary location to communicate with the UE, and (ii) MUS, where multiple UAVs

M. Banagar and H. S. Dhillon are with the Wireless@VT, Bradley Department of Electrical and Computer Engineering, Virginia Tech, Blacksburg, VA, USA (email: {mbanagar, hdhillon}@vt.edu), and A. F. Molisch is with the Wireless Devices and Systems Group, Ming Hsieh Department of Electrical and Computer Engineering, University of Southern California, Los Angeles, CA, USA (email: molisch@usc.edu). The support of the US NSF (Grants CNS-1923807 and CNS-1923601) is gratefully acknowledged.

are deployed at arbitrary locations to jointly communicate with the UE in a distributed-MIMO fashion. To isolate the effect of the UAV jitter, the UE is assumed to be static. The UAVs are assumed to be rotary-winged drones that are hovering at their locations. As shown in Fig. 1 for the SUS, the UAV is equipped with a single antenna (transceiver) which is located under the UAV platform with an offset of a_D meters from its centroid. We assume that the ground is aligned with the xy -plane while the UAV platform is located in the yz -plane and is initially parallel to the xy -plane at height $h = z_D$. The initial location of the transceiver is assumed to be $P_D(0) = (0, 0, z_D)$ and the locations of the UE and the n -th scatterer are denoted by $P_U = (x_U, y_U, 0)$ and $P_{S_n} = (x_{S_n}, y_{S_n}, z_{S_n})$, respectively (with the convention that $P_{S_0} \equiv P_U$). We represent the UAV-UE, UAV-scatterer, and scatterer-UE distances at time t by $d_0(t)$, $d_n(t)$, and $d_{S_n,U}$, respectively. The angle-of-departure (AoD) from the UAV to the UE and from the UAV to the n -th scatterer (measured w.r.t. the z -axis) are denoted by φ_0 and φ_n , respectively. Furthermore, the angle between the x -axis and the line connecting the origin to the projection of P_{S_n} onto the ground is denoted by ω_n .

We assume that the UAV may experience fluctuations due to the lack of robust and fixed infrastructure, wind gusts, and the high vibration frequency of its propellers and rotors [3], thus making it jitter. We model these fluctuations by random processes and study their impact on the received signal at the UE. Note that because of this jittering, the UAV platform may rotate in any of its three dimensions: roll, pitch, and yaw. In this letter, however, we only consider the pitch angle for simplicity. This pitch angle is denoted by $\theta(t)$ at time t .

In this letter, we assume a multi-path channel model where there is one LoS link between the UAV and the UE (the green solid lines in Fig. 1) and N multi-path components (MPCs) from scatterers (the red dotted lines for the n -th MPC in Fig. 1). In the SUS, we represent the received signal $r(t)$ at time t in the baseband (using the convention $d_{S_0,U} = 0$) as:

$$r(t) = \sum_{n=0}^N \alpha_n e^{-j \frac{2\pi}{\lambda} (d_n(t) + d_{S_n,U})}, \quad (1)$$

where $\lambda = \frac{c}{f_c}$ is the wavelength of the received signal, c is the speed of light, f_c is the carrier frequency, and α_0 and α_n are the amplitudes of the LoS link and the n -th MPC, respectively. Note that α_n and $d_n(t)$ may not be independent from each other in general. Similarly in the MUS, the received signal from the i -th UAV can be written as:

$$r_i(t) = \sum_{n=0}^N \alpha_{i,n} e^{-j \frac{2\pi}{\lambda} (d_{i,n}(t) + d_{S_n,U})}, \quad (2)$$

where $\alpha_{i,n}$ and $d_{i,n}(t)$ are the amplitude and distance from the i -th UAV to the n -th scatterer. The AoD from the i -th UAV to the n -th scatterer is denoted by $\varphi_{i,n}$.

Remark 1. For ease of notation, we assume that the antenna gain is constant within the range of interest for the angles of the MPCs. For a reasonably smooth amplitude antenna pattern $G(\varphi)$ and assuming small pitch angle, a nonuniform antenna pattern would only require multiplication of α_n with $G(\varphi_n)$.

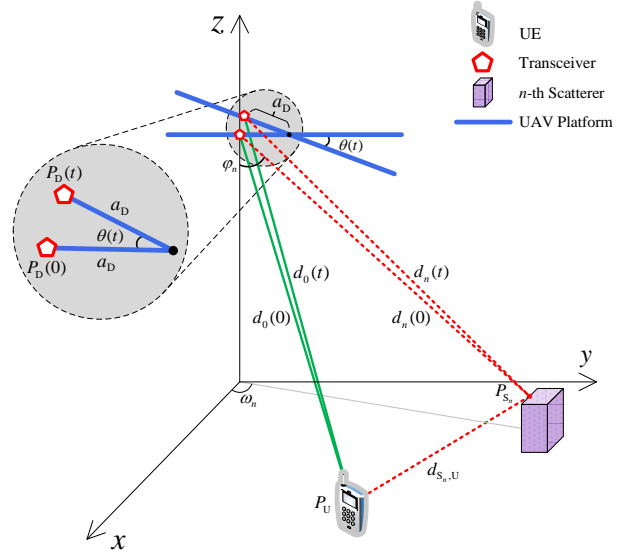


Fig. 1. An illustration of the system model. The green solid lines represent the LoS links from the UAV transceiver to the UE at times 0 and t and the red dotted lines represent the MPCs from the scatterers.

Remark 2. Due to the high carrier frequency of the received signal ($f_c = 1 \sim 6$ GHz), the wavelength will be in the order of centimeters ($\lambda = 5 \sim 30$ cm). Hence, a small variation in the UAV-UE distance may cause a large phase offset. Note that this effect is even more pronounced at mmWave frequencies.

We now introduce the coherence time (T_C) of the channel as the main metric of interest in this letter. Coherence time is defined as the first instant when the channel ACF drops below a certain threshold γ [15].

III. CHANNEL AUTOCORRELATION FUNCTION

In this section, we present a comprehensive analysis of the channel ACF for both the SUS and the MUS. We begin our analysis by deriving the relation between the pitch angle ($\theta(t)$) and the difference between the UAV-scatterer (or UAV-UE) distances ($d_{D,n}(t) = |d_n(t) - d_n(0)|$) in the following lemma.

Lemma 1. For a jittering UAV, reasonably assuming $a_D \ll d_n(t)$ and $\theta(t) \ll 1$ rad, we have $d_{D,n}(t) \approx a_D \cos(\varphi_n) \theta(t)$.

Proof: As shown in Fig. 1, when the UAV jitters, the location of the transceiver changes from $P_D(0) = (0, 0, z_D)$ to $P_D(t) = (0, a_D(1 - \cos(\theta(t))), z_D + a_D \sin(\theta(t)))$. We now write the equations for $d_n(0)$ and $d_n(t)$ as follows:

$$\begin{aligned} d_n(0) &= \sqrt{x_{S_n}^2 + y_{S_n}^2 + (z_{S_n} - z_D)^2}, \\ d_n(t) &= \sqrt{x_{S_n}^2 + [y_{S_n} - a_D(1 - \cos \theta(t))]^2 + [z_{S_n} - z_D - a_D \sin \theta(t)]^2} \\ &\stackrel{(a)}{\approx} \sqrt{x_{S_n}^2 + y_{S_n}^2 + (z_{S_n} - z_D)^2 - 2a_D[y_{S_n}(1 - \cos \theta(t)) + (z_{S_n} - z_D) \sin \theta(t)]} \\ &\stackrel{(b)}{\approx} d_n(0) - \frac{a_D[y_{S_n}(1 - \cos \theta(t)) + (z_{S_n} - z_D) \sin \theta(t)]}{d_n(0)}, \end{aligned}$$

where in (a) we used $a_D \ll y_{S_n}$ and in (b) we used the approximation $\sqrt{1 - \beta} = 1 - \frac{\beta}{2}$ for small β . Using $d_n(0) =$

$(z_D - z_{S_n})/\cos(\varphi_n)$, we write the distance difference as:

$$\begin{aligned} d_{D,n}(t) &\approx \frac{a_D \cos(\varphi_n)}{z_D - z_{S_n}} [(z_D - z_{S_n}) \sin \theta(t) - y_{S_n}(1 - \cos \theta(t))] \\ &\stackrel{(a)}{=} a_D \cos(\varphi_n) \sin \theta(t) - a_D \sin(\omega_n) \sin(\varphi_n)(1 - \cos \theta(t)) \\ &\approx a_D \cos(\varphi_n) \theta(t) - a_D \sin(\omega_n) \sin(\varphi_n) \frac{\theta^2(t)}{2} \\ &\approx a_D \cos(\varphi_n) \theta(t), \end{aligned} \quad (3)$$

where in (a) we used $y_{S_n}/(z_D - z_{S_n}) = \tan(\varphi_n) \sin(\omega_n)$ and the last two steps result from the small-angle approximation of the pitch angle ($\theta(t) \ll 1$ rad). ■

A. ACF Analysis in the SUS

We present the main result of this letter in the following theorem.

Theorem 1. *The channel ACF for a jittering UAV in a multi-path channel is approximated as:*

$$R(\tau) \approx \sum_{n=0}^N \mathbb{E} \left[|\alpha_n|^2 e^{j \frac{2\pi}{\lambda} a_D \cos(\varphi_n) \theta(\tau)} \right]. \quad (4)$$

Proof: Assuming that $r(t)$ is a wide-sense stationary (WSS) process, we write the channel ACF using (1) as follows:

$$\begin{aligned} R(\tau) &= \mathbb{E}[r(t)r^*(t+\tau)] \\ &= \mathbb{E} \left[\sum_{m=0}^N \sum_{n=0}^N \alpha_m \alpha_n^* e^{j \frac{2\pi}{\lambda} (d_n(t+\tau) - d_m(t))} e^{j \frac{2\pi}{\lambda} (d_{S_n, U} - d_{S_m, U})} \right] \\ &= \sum_{m=0}^N \sum_{\substack{n=0 \\ n \neq m}}^N \mathbb{E} \left[\alpha_m \alpha_n^* e^{j \frac{2\pi}{\lambda} (d_n(t+\tau) - d_m(t))} \right] \mathbb{E} \left[e^{j \frac{2\pi}{\lambda} (d_{S_n, U} - d_{S_m, U})} \right] \\ &\quad + \sum_{n=0}^N \mathbb{E} \left[|\alpha_n|^2 e^{j \frac{2\pi}{\lambda} d_{D,n}(\tau)} \right], \end{aligned}$$

where the double summation in the last equality is zero since the random variable $\left[\frac{d_{S_n, U} - d_{S_m, U}}{\lambda} \bmod 1 \right]$ is uniformly distributed from 0 to 1 [16, Lemma 4]. Hence, using Lemma 1, we obtain the final result. ■

One can compute (4) by first conditioning on φ_n , evaluating the resulting expectation, and then deconditioning for a given distribution of φ_n . While the result in (4) is general since it holds for any angular power spectrum model, we need to specialize it for a specific model in order to be able to obtain further insights. For that, we will use the well-accepted Laplacian model for the power of the n -th MPC [17], [18], which is given as $|\alpha_n|^2 = \frac{1}{2\sigma} e^{-\frac{|\varphi_n - \varphi_0|}{\sigma}}$, $1 \leq n \leq N$, where σ is the scale parameter of the Laplacian model. In this letter, we use the Rician multi-path fading channel model with factor K to capture the higher probability of LoS in aerial networks.

Corollary 1. *Assuming the Laplacian angular power spectrum with $|\alpha_0|^2 = K \sum_{n=1}^N |\alpha_n|^2 = K \sum_{n=1}^N \frac{1}{2\sigma} e^{-\frac{|\varphi_n - \varphi_0|}{\sigma}}$, the channel ACF is simplified as:*

$$R(\tau) \approx \mathbb{E} \left[|\alpha_0|^2 e^{j \frac{2\pi}{\lambda} a_D \cos(\varphi_0) \theta(\tau)} \right] +$$

$$\sum_{n=1}^N \mathbb{E} \left[\frac{1}{2\sigma} e^{-\frac{|\varphi_n - \varphi_0|}{\sigma}} e^{j \frac{2\pi}{\lambda} a_D \cos(\varphi_n) \theta(\tau)} \right]. \quad (5)$$

As mentioned in the previous section, due to the UAV jittering, we model the variations in the pitch angle by random processes. Note that the UAV jittering imposes an *effective Doppler shift* of $f_D = \frac{a_D \cos(\varphi_0) \dot{\theta}(\tau)}{\lambda \tau}$ on the channel. In this letter, we use two different random processes for this purpose: (i) the Wiener process, and (ii) the sinusoidal process. Note that one can also consider more complex random processes, such as the Gauss-Markov process, to analyze the coherence time of the channel but as is often the case in analysis, the additional complexity obfuscates key design insights.

Remark 3. (No Jitter). *In an ideal setting where the UAV platform is “completely” stable without any jitter or angular deviations, we have $\theta(\tau) = 0$ which results in a constant value for $R(\tau)$ for all τ . As expected, the coherence time will be infinity in this case.*

1) *Wiener Process:* The fundamental properties of a Wiener process W_t can be summarized as follows: (i) $W_0 = 0$, (ii) W_t has independent increments, (iii) W_t has Gaussian increments, (iv) W_t is continuous in t . Assuming $\theta(\tau)$ to be a Wiener process, one can show that its probability density function (pdf) follows a Gaussian distribution with mean zero and variance τ . Hence,

$$\begin{aligned} R(\tau) &\approx \sum_{n=0}^N \mathbb{E} \left[|\alpha_n|^2 \mathbb{E} \left[e^{j \frac{2\pi}{\lambda} a_D \cos(\varphi_n) \theta(\tau)} \right] \right] \\ &= \sum_{n=0}^N \mathbb{E} \left[|\alpha_n|^2 e^{-\left(\frac{2\pi^2}{\lambda^2} a_D^2 \cos^2(\varphi_n) \right) \tau} \right], \end{aligned} \quad (6)$$

where the last equality results from the characteristic function (CF) of a Gaussian random variable. This result shows that the channel ACF becomes an exponentially decaying function of τ when $\theta(\tau)$ is modeled as a Wiener process, which severely affects the coherence time of the channel. Further discussion on this result is provided in Section IV.

2) *Sinusoidal Process:* In this case, we assume that the pitch angle is given by:

$$\theta(\tau) = A \sin(2\pi F \tau), \quad (7)$$

where A and F are independent random variables representing the amplitude and the frequency of the pitch angle variations, respectively. Assuming $A \sim U[-\theta_m, \theta_m]$ and $F \sim p_F(f)$, where θ_m is the maximum pitch angle and $p_F(\cdot)$ is some given pdf, one can simplify (4) to obtain the channel ACF as follows:

$$\begin{aligned} R(\tau) &\approx \sum_{n=0}^N \mathbb{E} \left[|\alpha_n|^2 e^{j \frac{2\pi}{\lambda} a_D \cos(\varphi_n) A \sin(2\pi F \tau)} \right] \\ &= \sum_{n=0}^N \mathbb{E} \left[|\alpha_n|^2 \int_{-\infty}^{\infty} \text{sinc}\left(\frac{2}{\lambda} a_D \cos(\varphi_n) \theta_m \sin(2\pi f \tau)\right) p_F(f) df \right], \end{aligned} \quad (8)$$

where $\text{sinc}(x) = \frac{\sin(\pi x)}{\pi x}$ and in the last equality, we used the CF of the uniform random variable and then took the expectation w.r.t. F . Note that $R(\tau)$ is not a periodic function of τ due to the random frequency of the pitch angle. However,

if we assume a constant F , then $R(\tau)$ will be periodic in τ even with a random pitch angle amplitude A .

Using (6) and (8), we can now derive the coherence time of the channel for each random process as follows:

$$T_C = \min\{\tau : R(\tau) \leq \gamma\}. \quad (9)$$

Explicitly for the Wiener process, using $N = 0$ (an LoS channel) with an arbitrary non-random AoD, the coherence time of the channel can be written in closed-form as:

$$T_C = -\frac{\lambda^2}{2\pi^2 a_D^2 \cos^2(\varphi_0)} \log\left(\frac{\gamma}{|\alpha_0|^2}\right). \quad (10)$$

For the sinusoidal process, on the other hand, the closed-form solution is not available and we need to numerically solve (8) to obtain the coherence time of the channel.

B. ACF Analysis in the MUS

In this model, we assume that M UAVs form a distributed MIMO transceiver to jointly communicate with the UE. The channel autocorrelation matrix can be written as:

$$\mathbf{R}(\tau) = [R_{ik}(\tau)]_{1 \leq i, k \leq M} = \mathbb{E}[\mathbf{r}(t)\mathbf{r}^*(t + \tau)],$$

where $\mathbf{r}(t) = [r_1(t), r_2(t), \dots, r_M(t)]^T$ is the received signal vector which is assumed to be WSS, and $R_{ik}(\tau)$ is the (i, k) -th element of $\mathbf{R}(\tau)$.

Theorem 2. *The channel autocorrelation matrix for M jittering UAVs that form a distributed MIMO transceiver in an environment with one LoS link for each UAV and N MPCs can be approximated as:*

$$\mathbf{R}(\tau) \approx \text{diag} \left\{ \sum_{n=0}^N \mathbb{E} \left[|\alpha_{i,n}|^2 e^{j \frac{2\pi}{\lambda} a_D \cos(\varphi_{i,n}) \theta(\tau)} \right] \right\}. \quad (11)$$

Proof: For the diagonal elements of $\mathbf{R}(\tau)$, Theorem 1 is directly applied and we have:

$$R_{ii}(\tau) = \mathbb{E}[r_i(t)r_i^*(t + \tau)] \approx \sum_{n=0}^N \mathbb{E} \left[|\alpha_{i,n}|^2 e^{j \frac{2\pi}{\lambda} a_D \cos(\varphi_{i,n}) \theta(\tau)} \right].$$

On the other hand, for the off-diagonal elements, we can write:

$$\begin{aligned} R_{ik}(\tau) &= \mathbb{E}[r_i(t)r_k^*(t + \tau)] \\ &= \mathbb{E} \left[\sum_{m=0}^N \sum_{n=0}^N \alpha_{i,m} \alpha_{k,n}^* e^{j \frac{2\pi}{\lambda} (d_{k,n}(t+\tau) - d_{i,m}(t))} e^{j \frac{2\pi}{\lambda} (d_{S_n,U} - d_{S_m,U})} \right] \\ &= \sum_{n=0}^N \mathbb{E} \left[\alpha_{i,n} \alpha_{k,n}^* e^{j \frac{2\pi}{\lambda} (d_{k,n}(t+\tau) - d_{k,n}(t))} \right] \mathbb{E} \left[e^{j \frac{2\pi}{\lambda} (d_{k,n}(t) - d_{i,n}(t))} \right] + \\ &\quad \sum_{m=0}^N \sum_{\substack{n=0 \\ n \neq m}}^N \mathbb{E} \left[\alpha_{i,m} \alpha_{k,n}^* e^{j \frac{2\pi}{\lambda} (d_{k,n}(t+\tau) - d_{i,m}(t))} \right] \mathbb{E} \left[e^{j \frac{2\pi}{\lambda} (d_{S_n,U} - d_{S_m,U})} \right], \end{aligned}$$

where in the first summation of the last equality we used the fact that the jitter in the location of UAVs is independent of the distances between the UAVs and the scatterers (or the UE). Hence, since the random variable $\left[\frac{d_{k,n}(t) - d_{i,n}(t)}{\lambda} \bmod 1 \right]$ is uniformly distributed from 0 to 1 [16, Lemma 4], we conclude that this summation is zero. The second summation is also zero using a similar reasoning as in the proof of Theorem 1. ■

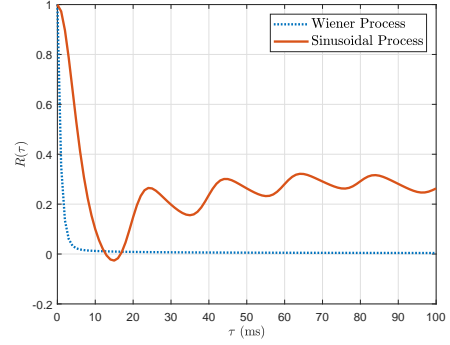


Fig. 2. The channel ACF for different models. The parameters are $f_c = 6$ GHz and $\theta_m = 5^\circ$.

Corollary 2. *Assuming the Laplacian angular power spectrum with Rician fading model, the channel autocorrelation matrix is simplified as follows:*

$$\begin{aligned} \mathbf{R}(\tau) &\approx \text{diag} \left\{ \mathbb{E} \left[|\alpha_{i,0}|^2 e^{j \frac{2\pi}{\lambda} a_D \cos(\varphi_{i,0}) \theta(\tau)} \right] \right\} + \\ &\quad \sum_{n=1}^N \text{diag} \left\{ \mathbb{E} \left[\frac{1}{2\sigma} e^{-\frac{|\varphi_{i,n} - \varphi_{i,0}|}{\sigma}} e^{j \frac{2\pi}{\lambda} a_D \cos(\varphi_{i,n}) \theta(\tau)} \right] \right\}. \quad (12) \end{aligned}$$

Similar to the SUS, one can model the random process $\theta(\tau)$ using the Wiener or sinusoidal processes to obtain the channel autocorrelation matrix. The fundamental observation in the MUS is that when multiple UAVs are hovering at some locations to communicate with the UE in a distributed-MIMO fashion, then the channels will be uncorrelated from each other. Using (9) and (11), we conclude that the coherence time of the channel in the MUS is the same as that of the SUS.

IV. SIMULATION RESULTS

In this section, we present numerical results to demonstrate the impact of UAV jittering on the coherence time of the channel. We assume that a single rotary-winged UAV hovers at some arbitrary location and jitters based on either the Wiener or sinusoidal processes. For the number of scatterers, we assume $N = 20$ and $N = 10$ in the sub-6 GHz and mmWave frequencies, respectively. Following Corollary 1, we assume a Laplacian angular power spectrum with $K = 6.5$ [19], $\varphi_0 = 20^\circ$ and $\sigma = 1$. For the sinusoidal process, we assume that the amplitude and frequency of the pitch angle both follow the uniform distribution, i.e., $A \sim U[-\theta_m, \theta_m]$ and $F \sim U[5, 25]$. Other parameters are $a_D = 40$ cm, $\theta_m = \{5, 7, 10\}^\circ$ [20], and $f_c = \{2.4, 6, 30\}$ GHz (equivalently, $\lambda = \{12.5, 5, 1\}$ cm).

In Fig. 2, we show the impact of UAV jittering on the channel ACF for both random processes where $f_c = 6$ GHz and $\theta_m = 5^\circ$. Assuming $\gamma = 0.5$, the coherence time of the channel is 771 μ s and 5.25 ms for the Wiener and sinusoidal processes, respectively. Although it was expected that the channel decorrelates with itself rapidly in the Wiener process, and thus has a very low coherence time, it is interesting to note that the coherence time for the sinusoidal model is not too high either. Hence, channel tracking and phase estimation for the proper symbol detection become very difficult [21].

In Figs. 3 and 4, we examine the sinusoidal model more carefully and demonstrate the impact of the carrier frequency

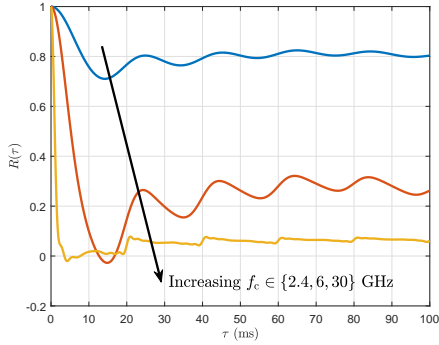


Fig. 3. The channel ACF when $\theta(\tau)$ follows the sinusoidal process with varying carrier frequencies and $\theta_m = 5^\circ$.

and the maximum pitch angle on the channel ACF and the coherence time. Obviously, as f_c or θ_m increase, the coherence time of the channel decreases. Assuming $\gamma = 0.5$, we observe that $T_C = \{\infty, 5.23, 0.989\}$ ms for $f_c = \{2.4, 6, 30\}$ GHz, respectively, when $\theta_m = 5^\circ$ (Fig. 3). Clearly, the coherence time of the channel will be in the order of microseconds for mmWave frequencies. Hence, the tracking of the channel and, in turn, communication is very challenging at the mmWave frequencies. From Fig. 4, we have $T_C = \{\infty, 12.78, 6.83\}$ ms for $\theta_m = \{5, 7, 10\}^\circ$, respectively, when $f_c = 2.4$ GHz. Consequently, in order to make the communication possible in higher frequencies and windy environments, we require UAVs with stabilizers that guarantee very low pitch angle deviations.

V. CONCLUSION

In this letter, we provided a rigorous mathematical analysis for the coherence time of the channel when UAVs experience random jittering. Assuming a Rician multi-path channel model, we considered two different scenarios for the number of UAVs communicating with the UE, i.e., SUS and MUS, and modeled the UAV jittering by random processes. For both the SUS and MUS, we formulated the channel ACF and derived the coherence time of the channel. Specifically in the MUS, we showed that the channels between the UAVs and the UE are uncorrelated from each other and the channel autocorrelation matrix is only determined by its diagonal elements. Our analysis demonstrated that even for small UAV jittering, the coherence time of the channel could be severely affected, thus making channel tracking and symbol detection difficult. A meaningful extension of this work is to study the impact of UAV jittering when the UAVs are *mobile* on the fundamental characteristics of the channel. Another direction for future work is to derive the coherence time of the channel in a concentrated MIMO scenario, i.e., having an antenna array instead of a single antenna in the UAV structure [12], [13].

REFERENCES

- [1] Y. Zeng, R. Zhang, and T. J. Lim, "Wireless communications with unmanned aerial vehicles: Opportunities and challenges," *IEEE Commun. Mag.*, vol. 54, no. 5, pp. 36–42, May 2016.
- [2] M. Mozaffari, W. Saad, M. Bennis, Y. Nam, and M. Debbah, "A tutorial on UAVs for wireless networks: Applications, challenges, and open problems," *IEEE Commun. Surveys Tuts.*, vol. 21, no. 3, pp. 2334–2360, 3rd Quart. 2019.

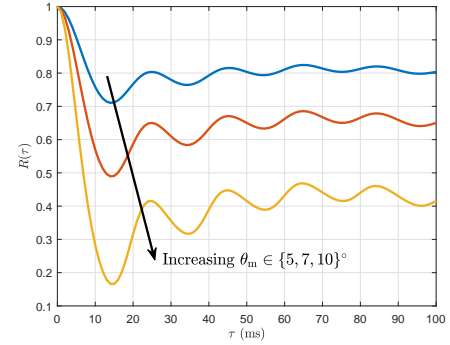


Fig. 4. The channel ACF when $\theta(\tau)$ follows the sinusoidal process with varying maximum pitch angles and $f_c = 2.4$ GHz.

- [3] Z. Li *et al.*, "Development and design methodology of an anti-vibration system on micro-UAVs," in *Proc. Int. Micro Air Veh. Conf. Flight Competition (IMAV)*, Sep. 2017, pp. 223–228.
- [4] M. Simunek, F. P. Fontan, and P. Pechac, "The UAV low elevation propagation channel in urban areas: Statistical analysis and time-series generator," *IEEE Trans. Antennas Propag.*, vol. 61, no. 7, pp. 3850–3858, 2013.
- [5] V. V. Chetlur and H. S. Dhillon, "Downlink coverage analysis for a finite 3-D wireless network of unmanned aerial vehicles," *IEEE Trans. Commun.*, vol. 65, no. 10, pp. 4543–4558, Oct. 2017.
- [6] R. Amer, W. Saad, and N. Marchetti, "Mobility in the sky: Performance and mobility analysis for cellular-connected UAVs," [Online]. Available: <http://arxiv.org/abs/1908.07774>, 2020.
- [7] M. Banagar and H. S. Dhillon, "Performance characterization of canonical mobility models in drone cellular networks," [Online]. Available: <http://arxiv.org/abs/1908.05243>, 2020.
- [8] —, "3GPP-inspired stochastic geometry-based mobility model for a drone cellular network," in *Proc. IEEE Global Commun. Conf. (GLOBECOM)*, Dec. 2019, pp. 1–6.
- [9] —, "Fundamentals of drone cellular network analysis under random waypoint mobility model," in *Proc. IEEE Global Commun. Conf. (GLOBECOM)*, Dec. 2019, pp. 1–6.
- [10] M. Banagar, V. V. Chetlur, and H. S. Dhillon, "Handover probability in drone cellular networks," *IEEE Wireless Commun. Lett.*, to appear.
- [11] M. T. Dabiri, H. Safi, S. Parsaeefard, and W. Saad, "Analytical channel models for millimeter wave UAV networks under hovering fluctuations," *IEEE Trans. Wireless Commun.*, to appear.
- [12] D. Xu, Y. Sun, D. W. K. Ng, and R. Schober, "Robust resource allocation for UAV systems with UAV jittering and user location uncertainty," in *Proc. IEEE Global Commun. Conf. (GLOBECOM) Workshops*, Dec. 2018, pp. 1–6.
- [13] —, "Multiuser MISO UAV communications in uncertain environments with no-fly zones: Robust trajectory and resource allocation design," *IEEE Trans. Commun.*, to appear.
- [14] H. Wu, Y. Wen, J. Zhang, Z. Wei, N. Zhang, and X. Tao, "Energy-efficient and secure air-to-ground communication with jittering UAV," *IEEE Transactions on Vehicular Technology*, to appear.
- [15] V. Va and R. W. Heath, "Basic relationship between channel coherence time and beamwidth in vehicular channels," in *Proc. IEEE 82nd Veh. Technol. Conf. (VTC'15-Fall)*, Sep. 2015, pp. 1–5.
- [16] H. S. Dhillon and G. Caire, "Wireless backhaul networks: Capacity bound, scalability analysis and design guidelines," *IEEE Trans. Wireless Commun.*, vol. 14, no. 11, pp. 6043–6056, Nov. 2015.
- [17] K. I. Pedersen, P. E. Mogensen, and B. H. Fleury, "Power azimuth spectrum in outdoor environments," *Electronics Lett.*, vol. 33, no. 18, pp. 1583–1584, Aug. 1997.
- [18] A. F. Molisch, *Wireless Communications*. Wiley-IEEE Press, 2011.
- [19] N. Goddemeier and C. Wietfeld, "Investigation of air-to-air channel characteristics and a UAV specific extension to the Rice model," in *Proc. IEEE Global Commun. Conf. (GLOBECOM) Workshops*, 2015, pp. 1–5.
- [20] B. Ahmed, H. R. Pota, and M. Garratt, "Flight control of a rotary wing UAV using adaptive backstepping," *Int. J. Robust Nonlinear Control*, vol. 20, no. 6, pp. 639–658, Apr. 2010.
- [21] M. Zhu *et al.*, "Tracking and positioning using phase information from estimated multi-path components," in *Proc. IEEE Int. Conf. Commun. (ICC) Workshops*, June 2015, pp. 712–717.